18-electron metals of the monosubstituted products.

One of the reviewers makes the point that the activation parameters in Table II support our contention that bridging carbonyls are progressively less stabilizing in the transition state in the order $Fe_3(CO)_{12} > Ru_3(CO)_{12} > Os_3(CO)_{12}$. It is suggested that the similarity of ΔH^* for the reaction of either $Fe_3(CO)_{12}$ or $Ru_3(CO)_{12}$ with PPh_3 reflects a similar attack by Me_3NO in both cases, but the more negative value of ΔS^* for the Ru system reflects the need for steric reorganization (perhaps, terminal CO → bridging CO). However, the larger ΔH^* and less negative ΔS^* for the reaction of $Os_3(CO)_{12}$ with PPh_3 may indicate that CO bridging is not important in the Os system.

Acknowledgment. We thank the United States–China Cooperative Science Program for the support of this collaborative research. The program is funded by the U.S. National Science Foundation and the PRC National Natural Science Foundation.

Registry No. $Fe_3(CO)_{12}$, 17685-52-8; $Ru_3(CO)_{12}$, 15243-33-1; $Os_3(CO)_{12}$, 15696-40-9; PPh_3, 603-35-0; $P(OPh)_3$, 101-02-0; $AsPh_3$, 603-32-7; $(CH_3)_3NO$, 1184-78-7.

Supplementary Material Available: Additional values are given of k_{obsd} for reactions (eq 2) at different concentrations of Me_3NO and different temperatures (Table S2) (3 pages). Ordering information is given on any current masthead page.

Intrinsic Barriers to Proton Exchange between Transition-Metal Centers: Application of a Weak-Interaction Model

Carol Creutz* and Norman Sutin*

Contribution from the Department of Chemistry, Brookhaven National Laboratory, Upton, New York 11973. *Received June 1, 1987*

Abstract: A weak-interaction model for proton self-exchange between transition-metal centers is considered. The rate constant obtained from the Fermi golden-rule expression of radiationless transition theory is a product of terms for assembling acid and base reactants at the correct orientation and distance, a classical reaction frequency, an electron–proton reaction probability, and classical nuclear factors deriving from the requirement for reorganization of ancillary ligands and solvent modes. It is found that such a model yields calculated rate constants and activation parameters in reasonable agreement with the experimental data, provided that the fluxionality of certain metal centers is taken into account.

Because proton transfer fulfills a central role in many processes, understanding and modeling of proton-transfer rates is an important challenge. Proton transfer between strongly electronegative centers such as oxygen or nitrogen is generally extremely rapid in solution[1] and proceeds via hydrogen-bonded "dimers" for which solid-state[2] and gas-phase species provide useful models. Recent ab initio calculations[3] accurately reproduce the properties of the gaseous ions and so provide a point of departure for modeling the dynamics of the proton transfer in this strong interaction limit. By contrast, although slow proton transfer to carbon centers has stimulated considerable experimental and theoretical activity,[4-6] there appears to be no consensus as to whether these reactions are better treated in terms of an adiabatic (strong-interaction)[5] or a nonadiabatic (weak-interaction) model.[6-9] Recent measurements of proton self-exchange rates[10] (eq 1) between transition-metal complexes in acetonitrile provide a basis for a critical

$$ML_nH + ML_n^- \rightarrow ML_n^- + ML_nH \quad (1)$$

Table I. Proton Self-Exchange Rates at 20–30 °C

	solvent	pK_a	k_{ex}, M^{-1} s^{-1}
$NH_4^+ + NH_3$	H_2O, 30 °C	9.1	1.3×10^9 [a]
$CH_3NH_3^+ + CH_3NH_2$	H_2O, 30 °C	10.5	0.4×10^9 [a]
$PhNH_3^+ + PhNH_2$	CH_3CN, 25 °C	10.5	$\geq 10^8$ [c]
$HFl + Fl^-$	Et_2O, 25 °C	--	2×10^{-5} [b]
$HM(cp)(CO)_3 + M(cp)(CO)_3^-$	CH_3CN, 25 °C		
M = Cr		13.3	1.8×10^4 [c]
M = Mo		13.9	2.5×10^3 [c]
M = W		16.1	6.5×10^2 [c]
$H_2Fe(CO)_4 + HFe(CO)_4^-$	CH_3CN, 25 °C	11.4	10^3 [c]
$H_2Os(CO)_4 + HOs(CO)_4^-$	CH_3CN, 25 °C	20.8	10^{-1} [c]

[a] Grunwald, E.; Ku, A. Y. *J. Am. Chem. Soc.* **1968**, *90*, 29. [b] HFl = a 9-substituted fluorene. Murdoch, J. R.; Bryson, J. A.; McMillen D. F.; Brauman, J. I. *J. Am. Chem. Soc.* **1982**, *104*, 600. [c] Jordan, R. F.; Norton, J. R. *J. Am. Chem. Soc.* **1982**, *104*, 1255. Edidin, R. T.; Sullivan, J. M.; Norton, J. R. *J. Am. Chem. Soc.* **1987**, *109*, 3945.

Table II. Properties of R–H Bonds

R–H	D_0, kcal mol^{-1}	ν_{R-H}, cm^{-1}	δ_{R-H}, cm^{-1}	$d°_{R-H}$, Å
M–H	50–75[a]	1600–2300[b]	600–900[b]	1.6–1.5[c,d]
				1.7–1.6[d,e]
				1.8–1.7[d,g]
N–H	80–100[f]	~3000[f]	~1500[f]	~1.0[f]
O–H	~110[f]	~3600[f]	~1300[f]	~1.1[f]
C–H	~100[f]	~3000[f]	~1300[f]	~0.98[f]

[a] Calderazzo, F. *Ann. N.Y. Acad. Sci.* **1983**, *415*, 37. Pearson, R. G. *Chem. Rev.* **1985**, *85*, 41. [b] Moore, D. S.; Robinson, S. D. *Q. Rev., Chem. Soc.* **1985**, 415. [c] For the first-transition series, left to right. [d] Teller, R. G.; Bau, R. *Struct. Bonding* **1981**, *44*, 1. [e] For the second-transition series, left to right. [f] Gordon, A. J.; Ford, R. A. *The Chemist's Companion*; Wiley: New York, 1972. [g] For the third-transition series, left to right.

(1) Eigen, M. F. *Angew. Chem., Int. Ed. Engl.* **1964**, *3*, 1.
(2) Hamilton, W. C.; Ibers, J. A. *Hydrogen Bonding in Solids*; Benjamin: New York, 1968.
(3) See e.g.: (a) Scheiner, S. *Acc. Chem. Res.* **1985**, *18*, 174. (b) del Bene, J. E.; Frisch, M. J.; Pople, J. A. *J. Phys. Chem.* **1985**, *89*, 3669. (c) Desmeules, P. J.; Allen, L. C. *J. Chem. Phys.* **1980**, *72*, 4731. (d) Perlet, P.; Peyerimhoff, S. D.; Bunker, R. J. *J. Am. Chem. Soc.* **1972**, *94*, 8301.
(4) (a) Bell, R. P. *The Proton in Chemistry*, 2nd ed.; Cornell Press: New York, 1973. (b) Bell, R. P. *The Tunnel Effect in Chemistry*; Chapman and Hall: London, 1980. (c) Kresge, A. J. *Acc. Chem. Res.* **1975**, *9*, 354–360. (d) Albery, W. J. *Annu. Rev. Phys. Chem.* **1980**, *31*, 227–263.
(5) Bell, R. P. *J. Chem. Soc., Faraday Trans. 2* **1980**, *76*, 954.
(6) (a) Dogonadze, R. R.; Kuznetsov, A. M.; Levich, V. G. *Sov. Electrochem.* **1967**, *3*, 648. (b) Dogonadze, R. R.; Kuznetsov, A. M.; Levich, G. *Electrochim. Acta* **1968**, *13*, 1025. (c) Levich, V. G.; Dogonadze, R. R.; German, E. D.; Kuznetsov, A. M.; Kharkats, Y. I. *Electrochim. Acta* **1970**, *15*, 353. (d) Dogonadze, R. R. In *Reactions of Molecules at Electrodes*; Hush, N. S., Ed.; Wiley: New York, 1971; p 135 ff. (e) German, E. D.; Kuznetsov, A. M. *J. Chem. Soc., Faraday Trans. 1* **1981**, *77*, 397. (f) Dogonadze, R. R.; Kuznetsov, A. M.; Marsagishvili, T. A. *Electrochim. Acta* **1980**, *25*. 1. (g) German, E. D.; Kuznetsov, A. M.; Dogonadze, R. R. *J. Chem. Soc., Faraday Trans. 2* **1980**, *76*, 1128. (h) German, E. D.; Kuznetsov, A. M. *J. Chem. Soc., Faraday Trans. 2* **1981**, *77*, 2203.
(7) (a) Ulstrup, J. *Charge Transfer Processes in Condensed Media*; Springer-Verlag: New York, 1979; pp 209–256. (b) Brüniche-Olsen, N.; Ulstrup, J. *J. Chem. Soc., Faraday Trans. 2* **1978**, *74*, 1690. (c) Brüniche-Olsen, N.; Ulstrup, J. *J. Chem. Soc., Faraday Trans. 1* **1979**, *75*, 205. (d) Sogaard-Andersen, P.; Ulstrup, J. *Acta Chem. Scand. Ser. A* **1983**, *37*, 585.

0002-7863/88/1510-2418$01.50/0 © 1988 American Chemical Society

examination of this issue for transition-metal centers. The rates of self-exchange reactions reflect the intrinsic kinetic barriers to reaction and such reactions are therefore the ideal point of departure for the testing of models. Here we consider a weak-interaction model.[6-9] The advantage of such a model is that the rate is related to the properties of the unperturbed reactants. An additional motivation for exploring the applicability of a weak-interaction model is that such a model provides a theoretical basis[6] for the Marcus H^+ and atom-transfer cross-relations[11] which have received attention in the organic literature[4d,12] and are presently being tested for transition-metal systems.[13] Here we find that the weak-interaction model, which is closely analogous to that which has been applied with great success to outer-sphere electron-transfer reactions,[14] can give good agreement with the experimental values for selected transition-metal hydride proton exchange reactions.

Experimental Systems. The proton self-exchange reaction eq 1, for which $\Delta G^\circ = 0$, will be the focus of this paper. In Table I bimolecular rate constants for proton self-exchange reactions are summarized. The rate constants determined by Jordan, Norton, and colleagues for neutral hydrido complexes may be compared with each other and with the few entries for nitrogen and carbon centers. The transition-metal-centered (M) exchanges are considerably slower than the nitrogen-centered exchanges and more rapid than the carbon-centered (fluorene) exchange. In addition, the M–H self-exchange rates span five orders of magnitude. The relative slowness of the M–H exchanges is particularly noteworthy in light of the bond properties summarized in Table II. The homolytic M–H bond energy is at least 25 kcal mol^{-1} less than typical NH, OH (or CH) bond energies. Both stretching and bending frequencies are considerably smaller for M–H. Indeed a typical M–H stretching force constant, 2 mdyn $Å^{-1}$ ($\sim$1900 cm^{-1}), is less than half those (4–6 mdyn $Å^{-1}$) characteristic of NH and OH bonds.

The relatively large (and variable) intrinsic barrier to M–H proton self-exchange has been attributed[10,15] to the large atomic and electronic configuration changes attending the proton transfer. In contrast to nitrogen and oxygen bases, the metal "lone-pair" electrons, which combine with the proton to yield the M–H bond, are not stereochemically active. Thus M-protonation generally results in a change of the coordination geometry about the metal, i.e., changes in the bond angles (as well as distances). This general feature is illustrated by the series[16] $Fe(CO)_4^{2-}$ (tetrahedral),[16a] $HFe(CO)_4^-$ (trigonal bipyramidal),[16b] and $H_2Fe(CO)_4$ (pseudooctahedral).[16c] Thus the requirement for nuclear configuration changes of the "spectator" (e.g., CO) ligands of the metal complex is expected to contribute to the activation barrier. An additional point of contrast between the transition-metal acids (hydrides) and bases and their oxygen-, nitrogen-, etc., centered counterparts is the tendency of the latter toward hydrogen bonding. There is no evidence for M–H··M^- (or M–H··X^-) hydrogen-bonding interaction.[17] Indeed the M–H bond polarity[18] and the M–H/M^- structural differences make such interactions unlikely. Both these features make the transition-metal hydrides[19] an attractive class for application of a weak-interaction model.

Proton Self-Exchange in Solution. The Weak-Interaction Model. For "simple"[20] proton self-exchange in solution the three-step mechanism shown in Scheme I is a convenient point of departure:

Scheme I

$$\text{M–H} + \text{M}^- \rightleftharpoons \text{M–H}|\text{M}^- \quad \text{(a)}$$

$$\text{M–H}|\text{M}^- \rightleftharpoons \text{M}^-|\text{M–H} \quad \text{(b)}$$

$$\text{M}^-|\text{M–H} \rightleftharpoons \text{M}^- + \text{M–H} \quad \text{(c)}$$

In step a, the acid and conjugate base diffuse together to form a precursor complex with M··M separation r; proton exchange occurs within this complex (step b) and is followed by dissociation of the successor complex in step c to yield separated products. In step b, rapid proton transfer, with first-order rate constant k_p^r, is favored by small r. However, the close approach of the reactants is opposed by repulsive interaction U^r (electron–electron repulsion, as well as other factors). Thus, for a given system, proton transfer will occur over a range of distances, with the bimolecular rate constant (k (M^{-1} s^{-1})) for the process being determined by the integral over separation distance r.

$$k\ (\text{M}^{-1}\ \text{s}^{-1}) = \int_0^\infty \frac{4\pi N r^2}{1000}[\exp(-U^r/RT)]Sk_p^r\,dr$$

(In the above expression, $S \leq 1$ is included as a statistical orientation factor since only certain M–H··M^- orientations lead to finite proton-transfer rates; N is Avogadro's number, R is the gas constant, T is the temperature, and r is expressed in cm.) As will be seen, the integrand in the above equations is significant only over a narrow range of distances between $\bar{r}$, the value at which the rate is maximal, and $\bar{r} + \delta r$. If we take δr as the width at half-height of the rate distribution and approximate the shape of the distribution as a triangle, then the bimolecular rate constant can be expressed as

$$k\ (\text{M}^{-1}\ \text{s}^{-1}) \simeq \frac{4\pi N \bar{r}^2 \delta r}{1000}[\exp(-U^r/RT)]Sk_p^r \quad (2)$$

For conceptual purposes it is useful to identify the first factor in eq 2 as an equilibrium constant for precursor-complex formation (step a in Scheme I), i.e.,

$$K_A^r\ (\text{M}^{-1}) = \frac{4\pi N \bar{r}^2 \delta r}{1000}[\exp(-U^r/RT)]S$$

then the bimolecular rate constant has the form

$$k\ (\text{M}^{-1}\ \text{s}^{-1}) = K_A^r k_p^r$$

(8) For a weak-interaction, golden-rule treatment of hydrogen atom transfer reactions see: Siebrand, W.; Wildman, T. A.; Zgierski, M. Z. *J. Am. Chem. Soc.* **1984**, *106*, 4083–4089, 4089–4096.

(9) (a) Jortner, J.; Ulstrup, J. *J. Am. Chem. Soc.* **1979**, *101*, 3744 (nonadiabatic atom transfer theory). (b) Jortner, J.; Ulstrup, J. *Chem. Phys. Lett.* **1979**, *63*, 236. (c) Buhks, E.; Jortner, J. *J. Chem. Phys.* **1985**, *83*, 4456. (d) Jortner, J. *Discuss. Faraday Soc.* **1982**, *74*, 271. (e) Buhks, E.; Navon, G.; Bixon, M.; Jortner, J. *J. Am. Chem. Soc.* **1980**, *102*, 2918.

(10) Jordan, R. F.; Norton, J. R. *J. Am. Chem. Soc.* **1982**, *104*, 1255; *ACS Symp. Ser.* **1982**, *198*, 403.

(11) (a) Marcus, R. A. *J. Phys. Chem.* **1968**, *72*, 891. (b) Cohen, A. O.; Marcus, R. A. *J. Phys. Chem.* **1968**, *72*, 4249. (c) Marcus, R. A. *J. Am. Chem. Soc.* **1969**, *91*, 7225. (d) Marcus, R. A. *Faraday Symp. Chem. Soc.* **1975**, *10*, 60. (e) Marcus, R. A. In *Tunneling in Biological Systems*; Chance, B., DeVault, D. C., Frauenfelder, H., Marcus, R. A., Schrieffer, J. B., Sutin, N., Eds.; Academic: New York, 1979; p 109.

(12) Dodd, J. A.; Brauman, J. I. *J. Am. Chem. Soc.* **1984**, *106*, 5356.

(13) Edidin, R. T.; Sullivan, J. M.; Norton, J. R. *J. Am. Chem. Soc.* **1987**, *109*, 3945.

(14) (a) Sutin, N. *Prog. Inorg. Chem.* **1983**, *30*, 441 and references cited therein. (b) Brunschwig, B. S.; Logan, J.; Newton, M. D.; Sutin, N. *J. Am. Chem. Soc.* **1980**, *102*, 5798.

(15) Walker, H. W.; Kresge, C.; Pearson, R. G.; Ford, P. C. *J. Am. Chem. Soc.* **1979**, *101*, 7428. Walker, H. W.; Pearson, R. G.; Ford, P. C. *J. Am. Chem. Soc.* **1983**, *105*, 1179.

(16) (a) Teller, R. G.; Chin, H. B.; Bau, R., unpublished results cited in: Chin, H. B.; Bau, R. *J. Am. Chem. Soc.* **1976**, *98*, 2434. (b) Smith, M. B.; Bau, R. *J. Am. Chem. Soc.* **1973**, *95*, 2388. (c) McNeill, E. A.; Scholer, F. R. *J. Am. Chem. Soc.* **1977**, *99*, 6243.

(17) (a) A possible exception to this statement is the trialkyl ammonium tetracarbonyl cobaltate ion-pair structure described by Calderazzo, et al.[17b] However, similar interactions are observed with other (non-proton-containing) cations such as sodium.[16b,17c] (b) Calderazzo, F.; Fachinetti, G.; Marchetti, F.; Zanazzi, P. F. *J. Chem. Soc., Chem. Commun.* **1981**, 181. (c) Darensbourg, M. Y. *Prog. Inorg. Chem.* **1985**, *33*, 221.

(18) Chen, H. W.; Jolly, W. L.; Kopf, J.; Lee, T. H. *J. Am. Chem. Soc.* **1979**, *101*, 2607.

(19) For recent reviews of the properties of hydrido complexes see: (a) Pearson, R. G. *Chem. Rev.* **1985**, *415*. (b) Moore, D. S.; Robinson, S. D. *Q. Rev., Chem. Soc.* **1984**, *415*. (c) Hlatky, G. G.; Crabtree, R. H. *Coord. Chem. Rev.* **1985**, *65*, 1. (d) Norton, J. R. In *Inorganic Reactions and Methods*; Zuckerman, J. J., Ed.; Verlag Chemie: Weinheim, 1987; Vol. 2, pp 204–235.

(20) (a) "Simple" in the sense that the metal coordination number changes by only one unit on protonation/deprotonation; systems that involve additional steps (e.g., the $Rh(CN)_4^{3-}$ + $HRh(CN)_5^{3-}$ exchange) will be discussed in a future publication. Also, special mechanisms such as hydride-to-carbonyl migration[20b] or electron transfer followed by H atom transfer[20c] are not considered here. (b) Narayanan, B. A.; Amatore, C.; Kochi, J. K. *Organometallics* **1987**, *6*, 129. (c) Bodner, G. S.; Gladysz, J. A.; Nielsen, M. F.; Parker, V. D. *J. Am. Chem. Soc.* **1987**, *109*, 1757.

in which the bimolecular rate constant is expressed as the product of an equilibrium constant and a first-order proton-transfer rate constant for step b in Scheme I.

As noted earlier, hydrogen is more electronegative than the transition-metal center. Thus the bond polarization in the reactant M–H and in the exchanged product is[19a]

$$\underset{\delta^+}{M}\!\!-\!\!\underset{\delta^-}{H}$$

However, the proton self-exchange reaction involves net H^+ transfer. In the present application of the weak-interaction model, proton motion is assumed to be rapid compared to the motion of other (heavier) nuclei. Thus the reactant M–H|M⁻ pair must achieve thermal activation of the classical (solvent and spectator ligand) modes prior to proton transfer so that energy is conserved in the relatively rapid proton-transfer step. At some close contact of the reactants, the overlap of the proton–metal vibrational wave functions is large enough for a finite proton-transfer probability. In addition, the reactant–product electronic coupling H_{AB} must be sufficient for H^+ transfer to occur at this nuclear configuration. In the weak (reactant–product; AB) interaction limit, the proton-exchange rate constant obtained from the Fermi golden-rule expression[6-9] of radiationless transition theory is eq 3 provided that the spectator-ligand and solvent energy surfaces are harmonic and that only the lowest metal–proton vibrational (0,0) states contribute significantly to the rate.

$$k\ (M^{-1}\ s^{-1}) = K_A{}^r k_p{}^r = K_A{}^r \nu_{el} \kappa_{ep}{}^r \kappa_{out}{}^r \kappa_L \tag{3}$$

$$\kappa_{ep}{}^r = \frac{2|H_{AB}{}^r|^2}{h\nu_{el}} \left[\frac{\pi^3}{(\lambda_{out}{}^r + \lambda_L)RT} \right]^{1/2} (FC)_{0,0}{}^r \tag{4}$$

$$\kappa_{out}{}^r = \exp(-\lambda_{out}{}^r/4RT) \tag{5}$$

$$\kappa_L = \exp(-\lambda_L/4RT) \tag{6}$$

The first-order proton-transfer rate constant $k_p{}^r$ is seen to be a product of a classical reaction frequency ν_{el} ($\sim 10^{13}$ s^{-1}), an electron–proton reaction probability κ_{ep}, and nuclear factors κ_{out} and κ_L deriving from the requirement for reorganization of solvent (outer-shell) and spectator-ligand modes, respectively. (In eq 4 $(FC)_{0,0}{}^r$ is the Franck–Condon factor for metal–proton vibrational overlap, discussed in the next section.) Here notation common in the treatment of electron-transfer processes has been used: $\lambda_{el} = \lambda_L + \lambda_{out}$ is the vertical free energy that would be required to transfer the proton from the hydride in its equilibrium (solvent and spectator-ligand) configuration to the base in its equilibrium configuration. In the limit of single-frequency, harmonic spectator-ligand and solvent free-energy surfaces the vertical λ values are related to the activation barriers ΔG^* by a factor of 4. Thus $\lambda_{el} = 4\Delta G_{el}{}^*$, $\lambda_{out} = 4\Delta G_{out}{}^*$, etc. Implicit in the above weak-interaction model is the assumption that the M–H frequency is sufficiently high that proton (fast) and classical (slow) motions may be treated independently.

While eq 3 arises from a consideration of the overlap of electronic and nuclear reactant–product wave functions,[21a] within this nonadiabatic model, reaction may be visualized as occurring by proton tunneling at a nuclear configuration determined by the classical modes (spectator-ligands and solvent) (see Figure 1); the probability of proton transfer depends upon the magnitude of the electronic coupling between initial and final states. Equation 3 is valid when the probability of reaction is low. This will be the case when both κ_{ep} (eq 4) and P_{el} (eq 7a) are much less than unity.[7a,9e] (The requirement that $P_{el} \ll 1$ is the more stringent condition; in general $\kappa_{ep} \ll 1$ when $P_{el} \ll 1$.) Here $h\nu_p$ is the

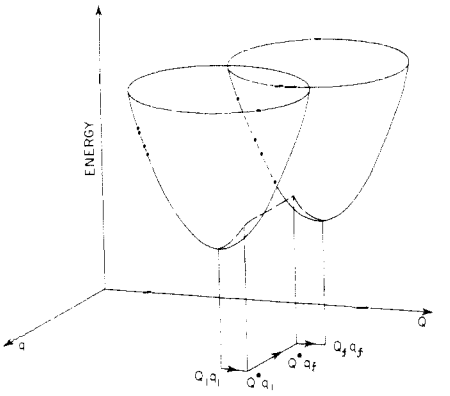

Figure 1. Energy of the reactant (front "cone") and product (rear "cone") M–H|M⁻ pairs as a function of classical Q_i and proton q_i nuclear coordinates. Starting from an equilibrium reactant pair configuration, activation occurs along the classical coordinate (solvent and ancillary ligand modes; $Q_i q_i \rightarrow Q^* q_i$), and the proton is transferred ($Q^* q_i \rightarrow Q^* q_f$) at constant energy, followed by relaxation of the classical modes ($Q^* q_f \rightarrow Q_f q_f$) to the equilibrium values for the product pair. (Adapted from ref 6e).

$$P_{el} = \frac{2|H_{AB}{}^r|^2}{h\nu_p} \left(\frac{\pi^3}{\lambda_p RT} \right)^{1/2} \ll 1 \tag{7a}$$

energy of the M–H stretch and $\lambda_p/4$ is the height of the barrier under which the proton "tunnels" (discussed later). In reality, H_{AB} is unlikely to be sufficiently small for P_{el} to be $\ll 1$ for most proton transfers of interest (unless the acid and base are constrained to be far apart). As a consequence, it is necessary to use a formalism for reactions that are electronically adiabatic, i.e., a formalism applicable to reactions in which the system remains on the lower (adiabatic) electronic surface throughout the course of the reaction. Reactions that are electronically adiabatic, but in which the vibrational overlaps are small, are referred to as "partially adiabatic".[7]

There are two approaches to the description of partially adiabatic reactions. In the first, the electronic contribution is "disregarded" (except for its effect in lowering the activation barrier), and the actual proton transfer is treated as a barrier penetration with use of a traditional tunneling formalism: effectively, $|H_{AB}|^2(FC)_{0,0}$ in eq 4 is replaced by $(h\nu_p)^2 \exp(-\sigma)$ where σ, the tunneling factor, is generally calculated from the Gamov formula.[6,7] In the second approach, the radiationless transition formalism is retained, κ_{ep} in eq 4 is factored into electronic (κ_{el}) and nuclear (κ_p) contributions, and the κ_{el} is then made adiabatic with use of the Landau–Zener expression, eq 7b. It is evident

$$\kappa_{el} = \frac{2[1 - \exp(-P_{el}/2)]}{2 - \exp(-P_{el}/2)} \tag{7b}$$

that $\kappa_{el} \rightarrow 1$ at large H_{AB} (electronically adiabatic) and that $\kappa_{el} \rightarrow P_{el}$ at small H_{AB} (electronically nonadiabatic).

The second approach parallels that used to describe tunneling of the high-frequency nuclear modes in adiabatic electron-transfer processes.[14b] It is appropriate when H_{AB} is sufficiently large that the reaction is electronically adiabatic, but not so large that a description in terms of the properties (force constants, bond distances) of the unperturbed reactants becomes inappropriate. When these conditions are satisfied, κ_{ep} ($=\kappa_p$) for the electronically adiabatic proton-transfer case is given by[21b,c] eq 8. Substitution

(21) (a) Note that, because it incorporates only reactant–product properties, eq 3 applies equally to H^+, H atom, and H^- transfer. Although different rates would be calculated as a result of differing H_{AB}, λ_L, and λ_{out} values for the three processes, the $(FC)_{0,0}$ terms are the same for all three processes (at a given r). In reality H atom transfer may require a strong interaction model as the M–H·M transition state is expected to be more bonding (M···H···M) than M–H M⁻. (b) Note that P_{el} in ref 14b is defined in terms of the classical limit, that is, in terms of ν_n, the effective (high-temperature) vibration frequency, and $\Sigma\lambda_n$, the sum of the λ values for the different modes. However, this difference is not important for the systems considered here since $\nu_n \sim \nu_p$ and $\Sigma\lambda_n \sim \lambda_p$. (c) Equation 8 is based on the assumption that the P_{el} to be substituted into the Landau–Zener expression (eq 7b) is given by eq 7a. On the other hand, if it is assumed that P_{el} is given by the factor multiplying $(FC)_{0,0}$ in eq 4, then $\kappa_{ep} = (FC)_{0,0}$. The latter assumption seems to have been made in obtaining eq 4 in ref 7c. The expressions for k_p in the present paper (eq 9) and in ref 7c (eq 4) thus differ by the factor $(\nu_p/\nu_{el})(\lambda_p/\lambda_{el})^{1/2}$ and yield rates that differ by about an order of magnitude. (d) At first sight it might appear that the two approaches considered here should lead to very different rate expressions. However, it can be shown[7a,9b] that, for Gamov tunneling through a parabolic barrier, the two approaches yield very similar expressions for the exponential factor in the low-temperature rate constant expression.

$$\kappa_{ep} = \frac{\nu_p}{\nu_{cl}}\left(\frac{\lambda_p}{\lambda_{cl}}\right)^{1/2}(FC)_{0,0}{}^r \ll 1 \quad (8)$$

of eq 8 into eq 3 yields eq 9, the rate constant for partially adiabatic proton transfer.[21d] (As before, the reaction is assumed to involve

$$k\ (M^{-1}\ s^{-1}) = K_A{}^r\nu_p(\lambda_p/\lambda_{cl})^{1/2}(FC)_{0,0}{}^r \exp[-(\lambda_{cl}/4 - H_{AB}{}^r)/RT] \quad (9)$$

only the lowest proton vibrational level.) In what follows we first discuss the distance dependence of the factors in eq 3 and 9 then consider under what conditions the partially adiabatic limit is expected to apply. Finally we turn to specific systems and the evaluation of λ_L.

Distance Dependence

Metal–Proton Overlap. In order to focus on the actual proton-transfer step and its sensitivity to reactant separation, we omit for the time being the role of solvent and ancillary ligand rearrangement; both are considered later. In evaluating the metal–proton overlap the critical distance parameter is $\Delta d°$, the distance over which the proton must transfer or tunnel; $\Delta d°$ is given by

$$\Delta d° = r_{M\cdot\cdot M} - 2d°_{M\text{-}H} \quad (10)$$

where $d°_{M\text{-}H}$ is the equilibrium M–H bond distance. If the proton transfer involves only the lowest reactant–product M–H vibrational levels (0,0) the Franck–Condon factor for harmonic oscillators is

$$(FC)_{0,0}{}^r = \exp(-\lambda_p{}^r/h\nu_p) \text{ with } \lambda_p{}^r = {}^1/_2 f_p(\Delta d°)^2 = \exp(-S)$$
$$\text{with } S = (1.49 \times 10^{-2})m_p(\nu_p, \text{cm}^{-1})(\Delta d°, \text{Å})^2 \quad (11)$$

where f_p is the force constant for the metal–hydride stretch and m_p is the "proton" mass (different for H and D, as is $h\nu_p$). The dependence of the Franck–Condon factor on $\Delta d°$ is shown in Figure 2 for the harmonic case (eq 11) with $h\nu_p = 1942$ cm^{-1} (line a) and $h\nu_p = 1765$ cm^{-1} (line b); also indicated (line c) is $(FC)_{0,0}$ for the Morse potential eq 12.[22] A homolytic bond energy D_0

$$E^r = D_0[1 - \exp(-\beta(\Delta d°))]^2 \quad (12)$$

$$\beta\ (\text{Å}^{-1}) = 1.218 \times 10^{-1}(h\nu_p, \text{cm}^{-1})[m_p/(D_0, \text{cm}^{-1})]^{1/2}$$

= 60 kcal mol^{-1} was used for line c on the assumption that the M–H stretch $h\nu_p$ for which the Franck–Condon factor is evaluated most closely resembles homolysis (at least near the bottom of the potential well). In either treatment the metal–proton vibrational overlap decreases very rapidly with $\Delta d°$. The calculated Franck–Condon factor is relatively large only for $\Delta d° < 0.6$ Å. At such small distances the harmonic and anharmonic (Morse) potentials yield rather similar rate factors. While only $(FC)_{0,0}$ (determined by vibrational overlap between the lowest reactant and product levels) is shown, contributions to the rate from 1 to 0 reactant–product levels, as well as from the bending modes, can also be evaluated, but at "low" temperature they do not substantively alter the patterns shown in Figure 2 for small $\Delta d°$.

Repulsive Factor. While proton transfer is obviously favored by the increase in vibrational overlap at small separation, electron–electron repulsion (U^r) between M–H and M$^-$ also increases with diminishing separation. The repulsive factor is particularly difficult to model in general[5,6] and various potentials have been considered.[23] For transition-metal centers, the dearth of experimental data[24] adds to the problem. Here the repulsive term eq 13 is modeled in terms of the metal-bound hydrogen (H)/metal

$$\kappa_u{}^r = \exp(-U^r/RT) \quad (13)$$

anion (M$^-$) interaction. The H··M$^-$ separation

$$r_{H\cdot\cdot M} = d°_{M\text{-}H} + \Delta d°_{M\text{-}H}$$

is thus the relevant distance parameter. The steep distance dependence obtained for U^r is illustrated in Figure 3. The curve shown is based on[25] a Buckingham potential (eq 14) for the H··M$^-$ interaction with M a second transition series metal center. The

$$U^r = a\exp(-br_{H\cdot\cdot M}) - cr_{H\cdot\cdot M}{}^{-6} \quad (14)$$

M–H··M$^-$ parameters used are[25] $a = 6149$ kcal mol^{-1}, $b = 3.13$ Å^{-1}, and $c = 168$ kcal mol^{-1} Å^6 (van der Waals radii 1.5 and 2.6 Å for H and M, respectively). In Figure 4 the composite factors $\kappa_u(FC)_{0,0}$ are also shown for a model protio and deuterio hydride ($h\nu_H = 1790$ cm^{-1}). In order to obtain these, an M–H bond length of 1.7 Å and the repulsive curve in Figure 3 were used. Thus the profiles provide a guide for the Mo(cp)(CO)$_3$H or –D exchange. Because of the opposing distance dependences of $(FC)_{0,0}$ and κ_u, their product (and the rate constant) peaks sharply at some optimum distance. For both –H and –D exchanges the curves obtained are quite symmetric—rather Gaussian in appearance. While the integrals under the curves in Figure 4 could be evaluated more exactly, it is evident that approximating the distributions as triangles of height proportional to $(\kappa_u k_p)_{max}$ and half-width δr is a useful approximation. For the "system" considered the maximum product $\kappa_u(FC)_{0,0}$ lies in the range 10^{-8}–10^{-7}, $\Delta d°$ is ~0.5 Å, $r_{M\text{-}H} \sim 2.2$ Å, $r_{M\text{-}M} \sim 3.9$ Å, and δr, the characteristic reaction width, is ~0.2 Å.

Solvent. A small barrier to the proton transfer arises from the sudden transfer of charge Δz in a dielectric medium (λ_{out}). For the transition-metal exchanges in Table I, the following approach is taken: the M–H/M$^-$ reactant pair is approximated as a sphere of radius $a = a° + r_{M\cdot\cdot M}/2$ with

$$a° = d°_{M\text{-}C} + d°_{C\text{-}O} + 1.5\ \text{Å} \simeq 4.6\ \text{Å}$$

where 1.5 Å is the van der Waals radius of oxygen. For charge transfer between two sites separated by r and symmetrically located on the diameter of a sphere immersed in a dielectric continuum with optical and static dielectric constants D_{op} and D_s, respectively, λ_{out} is approximately given by[14] eq 15 provided that $r < a$ and $D_{op} \ll D_s$. The calculation of λ_{out} may now be approached in two different ways. (1) It might be considered that H$^+$ is transferred over the distance $r = \Delta d°$ with $\Delta z = +1$. (2) The metal may be regarded as the center of negative charge in the anion conjugate base. Then transfer of the H atom results in simultaneous transfer of negative charge $\Delta z = -1$ over the distance $r = r_{M\cdot\cdot M}$ from one metal center to the other. The first approach involves authentic H$^+$ transfer and the second involves simultaneous H-atom and "electron" transfer:

$$\lambda_{out}{}^r = (\Delta z)^2(1/D_{op} - 1/D_s)[r^2/2(a° + r_{M\cdot\cdot M}/2)^3] \quad (15)$$

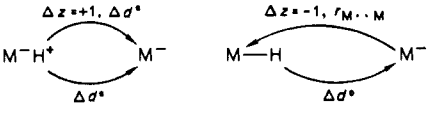

1 2

The first model does not accurately reflect the ground-state M–H properties: that is, M–H is not M$^-$H$^+$. Thus we adopt the second model and take $r = r_{M\cdot\cdot M}$. (Note that since the first model give negligible λ_{out} values because $r = \Delta d°$ is so small (eq 15), λ_{out} can only be overestimated by making this choice.) Then for acetonitrile solvent, $\Delta z = -1$ and $r = r_{M\cdot\cdot M}$, and λ_{out} is given by

$$\lambda_{out}{}^r = 86.7(r_{M\cdot\cdot M}{}^2/a^3)\ \text{kcal mol}^{-1}$$

(22) (a) Herzberg, G. *Spectra of Diatomic Molecules*, 2nd ed.; Van Nostrand Reinhold: New York; pp 99–101. (b) See the Appendix in ref 6h for the calculation of Franck–Condon factors with use of the Morse potential.

(23) Abraham, R. J.; Stolevik, R. *Chem. Phys. Lett.* **1978**, *58*, 622.

(24) (a) For example, note that van der Waals radii used in molecular mechanics calculations[25] (e.g., H, 1.5 Å; M, 2.6 Å) are generally much greater than traditionally tabulated values[24b] (H, 1.2 Å; M 1.6 Å). A van der Waals radius of 1.4 Å is derived for H if half the H··H distance in HMn(CO)$_5$ is taken.[24c] (b) Huheey, J. E. *Inorganic Chemistry: Principles of Structure and Reactivity*; Harper and Rowe: New York, 1972; pp 184–185. (c) LaPlaca, S. J.; Hamilton, W. C.; Ibers, J. A.; Davison, A. *Inorg. Chem.* **1969**, *8*, 1928.

(25) See: Boeyens, J. C. A.; Cotton, F. A.; Han, S. *Inorg. Chem.* **1985**, *24*, 1750. Boeyens, J. C. A. *Struct. Bonding* **1985**, *63*, 65.

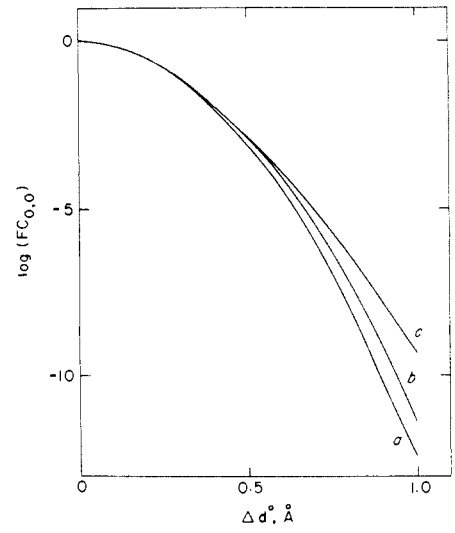

Figure 2. Metal–proton vibrational overlap as a function of distance; logarithm of the 0,0 Franck–Condon factor vs $\Delta d°$; (a) $h\nu_p$ = 1942 cm^{-1}, harmonic oscillator; (b) $h\nu_p$ = 1765 cm^{-1}, harmonic oscillator; (c) $h\nu_p$ = 1942 cm^{-1}, D_0 = 60 kcal mol^{-1}, β = 1.63 $Å^{-1}$, Morse function.

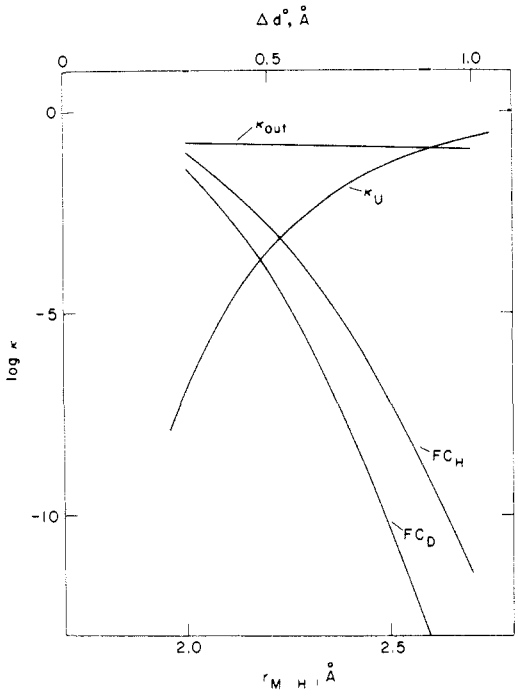

Figure 3. Distance dependences of the logarithm of the Franck–Condon factors for protio (FC_H) and deuterio (FC_D) harmonic oscillators with $h\nu_H$ = 1790 cm^{-1} and $h\nu_D$ = 1285 cm^{-1}, the repulsive term $\kappa_u = \exp(-U/RT)$, and the solvent term $\kappa_{out} = \exp(-\lambda_{out}/4RT)$ at 298 K for $d°_{M-H}$ = 1.7 Å ($r_{M..H} = \Delta d° + d_{M-H}$).

where the distances are in Å; for $r_{M..M}$ = 3.9 Å, λ_{out} = 4.7 kcal mol^{-1}. Over the separation range considered here λ_{out} is small and changes little. The distance dependence of κ_{out} is illustrated in Figure 3.

Although the exact magnitude obtained for λ_{out} cannot be taken too seriously,[26] λ_{out} is small because of the small distance over which charge transfer occurs even when r is taken as $r_{M..M}$.

(26) (a) The solvent treatment given in eq 15 is oversimplified in that the reactant pair has been treated as a hard sphere and the spacious cavities between the carbonyl ligands have been neglected. Ellipsoidal[26b] or more sophisticated spherical[26c] cavity models might be considered. In addition the use of the $1/D_{op} - 1/D_s$ function assumes that the charge transfer is rapid compared to all of the solvent dielectric relaxation processes except electronic relaxation—a debatable issue in itself. (b) Brunschwig, B. S.; Ehrenson, S.; Sutin, N. *J. Phys. Chem.* **1986**, *90*, 3657. (c) Brunschwig, B. S.; Ehrenson, S.; Sutin, N. *J. Phys. Chem.* **1987**, *91*, 4714.

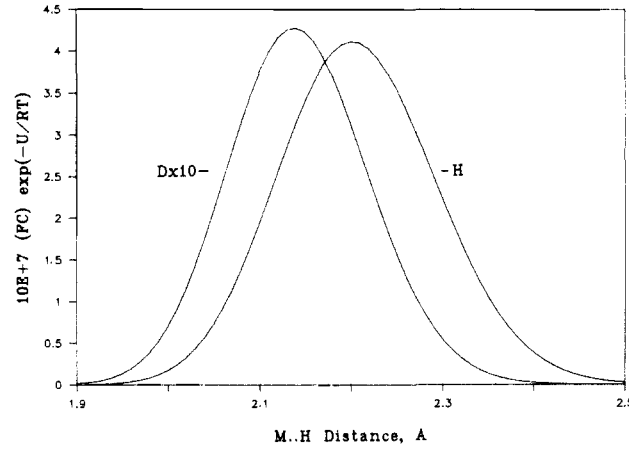

Figure 4. Distance dependence of the product $\kappa_u(FC)_{0,0}$ (see caption for Figure 3).

Table III. Summary of Calculated Rate Factors for an M–H/D + M^- Self-Exchange at 298 K[a]

	H	D
$d°_{M-H}$ (Å)	1.7	1.7
$h\nu_p$ (cm^{-1})	1790	1285
$\kappa_u(FC)_{0,0}$	4.1×10^{-7}	4.3×10^{-8}
$(FC)_{0,0}$	1.41×10^{-3}	7.55×10^{-4}
$\bar{r}_{M..H}$ (Å)	2.20	2.14
$r_{M..M}$ (Å)	3.90	3.84
$\Delta d°$ (Å)	0.50	0.44
δr(Å)	0.2	0.2
$4\pi Nr^2\delta r/1000$ (M^{-1})[b]	0.033	0.033
S	10^{-2}	10^{-2}
ν_{el} (s^{-1})	10^{13}	10^{13}
λ_{out} (kcal mol^{-1})	4.69	4.61
κ_{out}	0.14	0.14
λ_p (kcal mol^{-1})	33.5	25.9
U (kcal mol^{-1})	4.80	5.83
H_{AB} (kcal mol^{-1})[c]	(2.0)	(2.0)
k (M^{-1} s^{-1})	8.5×10^4	5.6×10^3
ΔH^* (kcal mol^{-1})	4.0	5.0
ΔS^* (cal mol^{-1} K^{-1})	-22.7	-24.8

[a] Calculated parameters refer to the maxima in Figure 4. [b] The "spherical" M–H and M^- complexes are taken to have van der Waals radii of 4.7 Å (typical values for mononuclear carbonyls). [c] Not calculated.

Because λ_{out} is relatively small, little solvent dependence of the exchange rates is likely to arise through dielectric-continuum contributions. Of course, in net proton-transfer reactions involving a partner capable of hydrogen bonding to the solvent, specific solvent effects should arise owing to the need to break reactant–solvent hydrogen bonds prior to reaction with the transition-metal center.

Orientational Factor. For the sake of completeness the orientational factor S was introduced in eq 2. As noted earlier $S \leq 1$ because only certain M–H/M^- orientations within the precursor complex (Scheme I) lead to a finite proton-transfer rate. The crude estimate $S = 10^{-2}$ used here is obtained from a simple geometric model: the metal hydride complex has a van der Waals radius of $a_{M-H} \sim 5$ Å and a surface area of $4\pi(a_{M-H})^2$. The van der Waals radius of H a_H is 1.5 Å and the fraction of the M–H sphere which is reactive with respect to proton transfer is $\pi(a_H)^2/4\pi(a_{M-H})^2 \sim 10^{-2}$ if *all* acceptor sites on "spherical" M^- are equivalent. These arguments are qualitative only since rotation rates and other competing steps are neglected.

Weak-Interaction Rate Constant in the Absence of Geometry Changes. The rate contributions considered above—metal–proton overlap, H··M^- repulsion, and solvent reorganization— are expected to be similar for a number of systems (especially for those in which bulky ligands are absent). Thus it is useful to estimate a weak-interaction rate constant for proton self-exchange between transition-metal centers in the absence of geometry changes. The relevant parameters are summarized in Table III. As outlined

earlier, the totally nonadiabatic rate constant is given by eq 3 and 4 when both κ_{el} and $\kappa_{ep} \ll 1$, and the partially nonadiabatic rate constant is given by eq 9 when $\kappa_{el} \sim 1$ and $\kappa_{ep} \ll 1$. First P_{el} (eq 7a) is considered: For the model system in Figure 4 the maximum value of the product $\kappa_u(FC)_{0,0}$ occurs at $\Delta d° \sim 0.5$ Å at which $\lambda_p = 33.5$ kcal mol^{-1}. From eq 7a, $P_{el} \ll 1$ for $H_{AB} \ll 2$ kcal mol^{-1}. At the rate maximum, $(FC)_{0,0}$ for the hydride is 1.4×10^{-3} and $\lambda_{out} = 4.7$ kcal mol^{-1}: consideration of eq 8 (with neglect of λ_L) then gives $\kappa_{ep} \ll 1$ for $H_{AB} \ll 13.4$ kcal mol^{-1} (4705 cm^{-1}). Although we cannot evaluate H_{AB}, we argue that for $\Delta d° = 0.5$ Å (at which distance $U^r = 4.8$ kcal mol^{-1}) it is unlikely that H_{AB} is much less than 2 kcal mol^{-1} (reaction totally nonadiabatic) and also unlikely that H_{AB} is as great as 13 kcal mol^{-1} (reaction totally adiabatic). Thus we use the partially nonadiabatic expression eq 9 to evaluate the rate constants. (To the extent that the requirement for angular changes (next section) increases λ_{el} the validity of taking $\kappa_{ep} \ll 1$ and eq 9 is only strengthened.) From eq 9 and the values summarized in Table III, $k_H = 3 \times 10^3$ M^{-1} s^{-1} if H_{AB} is neglected. For $H_{AB} = 2$ kcal mol^{-1}, $k_H = 8.5 \times 10^4$ M^{-1} s^{-1}. The corresponding values for the deuteride in Figures 3 and 4 are about a factor of 15 smaller.

The activation parameters at 298 K may be estimated from the following relations:

$$k = \nu_{el} \exp(\Delta S^*/R) \exp(-\Delta H^*/RT) \quad (16)$$

$$\Delta H^* = U + \lambda_{el}/4 - H_{AB} \quad (17)$$

$$\Delta S^* = R \ln \left(\frac{4\pi N r^2 S \delta r (\nu_p/\nu_{el})(\lambda_p/\lambda_{el})^{1/2}(FC)_{0,0}}{1000} \right) \quad (18)$$

(In eq 17, $\lambda_{el} = \lambda_{out}$ and $\lambda_{out} = 4\Delta G_{out}^*$ is treated as an enthalpy, i.e., $\Delta H_{out}^* = \lambda_{out}/4$ is assumed so that any temperature dependence of λ_{out} is neglected.) From eq 16–18, $\Delta H^* = 6.0 - H_{AB}$ kcal mol^{-1} and $\Delta S^* = -22.7$ cal deg^{-1} mol^{-1} for the hydride self-exchange; for the deuteride exchange $\Delta H^* = 7.0 - H_{AB}$ kcal mol^{-1} and $\Delta S^* = -24.8$ cal deg^{-1} mol^{-1}. Thus in a weak-interaction model the activation entropy is expected to be slightly more negative for the deuterio self-exchange than for the protio exchange, reflecting the smaller Franck–Condon factor for the former. The activation enthalpy is greater for D than for H because the rate maximum is at smaller separation so that the repulsive term is greater. Note that the above treatment is valid only to the extent that the position and width of the rate maxima in Figure 4 are temperature independent. In general, the activation parameters are not expected to be temperature independent over a wide range because the rate profile is determined by interaction between enthalpic (U^r and Boltzmann factors) and entropic (vibrational overlap) factors. However, with the parameters used in Figure 4, the calculated activation parameters change negligibly over the range 275–325 K.

Geometry Changes

Protonation of the transition-metal base is effectively an oxidative addition and the bonding in the product hydride complex is characteristic of the higher oxidation state (for protonation of M^-, the higher oxidation state is M^+). In contrast to outer-sphere, one-electron-transfer reactions of transition-metal complexes, in which the geometry changes involve largely bond-distance changes, the protonation of a transition-metal center is dominated by geometry (angular) changes. For example, consider an idealized organometallic ML_5H/ML_5^- system in which the acid is octahedral and the base is trigonal bipyramidal.

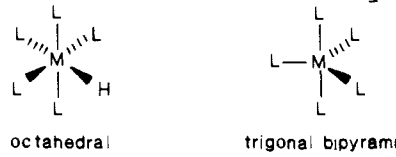

octahedral trigonal bipyramidal

If the proton is transferred to an equatorial site on the base, all of the angular changes occur in one plane and so are relatively simple to describe as shown in Scheme II. In the base, the L–M–L equatorial angles are 120° and, in the acid, 90°. If the proton were suddenly transferred from acid to base (requiring energy λ_L), distorted, vibrationally excited species A′ and D′ would result. The structural differences between D and D′ and A and A′ define the angular deformations required prior to the proton transfer (D* and A*) in the self-exchange reaction.

Scheme II

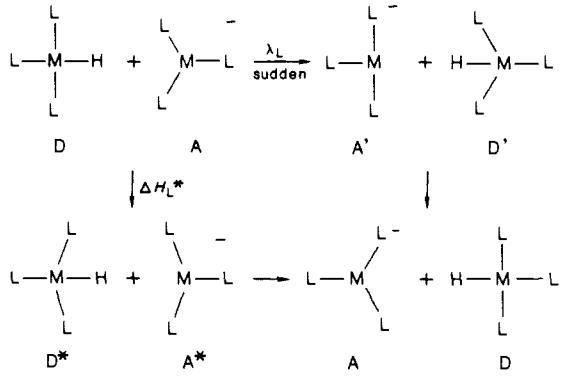

Several approaches to the treatment of the geometry changes are possible, with the approach to be used depending upon the nature of the system. First a harmonic oscillator treatment is introduced and illustrated. Following that a pre-equilibrium geometry change on the fluxional partner is considered.

Franck–Condon Harmonic-Oscillator Treatment. This approach is analogous to that applied to the symmetric stretch/compression modes critical to outer-sphere electron transfer of metal complexes[14] and has recently been applied to triatomic couples in which there are large geometry changes.[27] However, in proton exchange (or atom transfer, in general), unlike the above applications, the number of atoms or angles in the two reactants is not the same. As a consequence the motion relating reactants and products must be considered with some care and on a case by case basis.

To illustrate the application of this approach to the proton exchange we consider the PH_4^+/PH_3 self-exchange. Ideally a nonfluxional transition-metal MH_nH/MH_n^- exchange would be used as an example, but there are not sufficient data for such systems. The phosphonium–phosphine exchange does have features similar to the transition-metal systems in that P is (slightly) less electronegative than H and in that considerable geometric changes attend the exchange. For conceptual simplicity the metal–ligand (i.e., P–H) vibrations are described in terms of a simple valence force field[28]—that is, in terms of bond distances (r) and bond angles (θ) and force constants for bond stretching (f) and bond bending (h). Thus if the central atom of complex i is numbered 1 and the (monatomic) identical ligands 2, 3, ... the force field is of the form

$$2V_i = f_i(\Delta r_{12}^2 + \Delta r_{13}^2 + ...) + h_i[(\Delta\theta_{23})^2 + (\Delta\theta_{34})^2 + ...]$$

where Δr and $\Delta\theta$ are the displacements from the equilibrium values $r°$ and $\theta°$. In PH_3 the P–H bond distance $r°$ is 1.419 Å and the three H–P–H angles are 93.5°.[3c] In PH_4^+ the P–H distance is 1.415 Å and the six H–P–H angles are 109.5°.[29a] Stretching and bending force constants are 3.1[29b] and 3.1[29c] mdyn Å^{-1} and 0.58[29b] and 0.46[29c] mdyn Å rad^{-2} for PH_3 and PH_4^+, respectively. Consider that one (donor) PH_4^+ bond axis is colinear with the C_3 axis of the acceptor PH_3.

(27) Stanbury, D. M.; Lednicky, L. A. *J. Am. Chem. Soc.* **1984**, *106*, 2847.
(28) Herzberg, G. *Infrared and Raman Spectra*; Van Nostrand Reinhold: New York, 1945.
(29) (a) Sequeira, A.; Hamilton, W. C. *J. Chem. Phys.* **1967**, *47*, 1818. (b) These values differ slightly from those given by Herzberg (ref 28, p 177) because the original vallues were based on a smaller H–P–H angle in PH_3. (c) Calculated for PH_4^+ from $\nu_1 = 2295$ cm^{-1} and $\nu_2 = 1086$ cm^{-1} for stretching and bending force constants, respectively [Nakamoto, K. *Infrared and Raman Spectra of Inorganic and Coordination Compounds*, 3rd ed.; Wiley: New York, 1978; p 135], with use of the expressions on p 182 in ref 28.

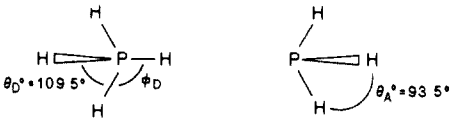

So that energy may be conserved in the actual proton transfer, bond lengths and angles must be identical at donor (D, PH_4^+) and acceptor (A, PH_3) sites: Thus $r_A = r_D = r^*$. In addition this equivalence requires a bending motion in which three PH_4^+ θ_D angles compress to θ^* and three PH_4^+ angles ϕ_D open to $\phi^* = \theta^\circ_D - g(\theta^* - \theta^\circ_D)/\sqrt{3}$. [Note that, in this motion, changes in $\Delta\theta$ and $\Delta\phi$ are related by $\Delta\phi \simeq -g(\Delta\theta)/\sqrt{3}$ where $g = \cos(\theta_D/2)/\cos(\phi) = 1.53$.] In PH_3 the angles θ_A open to θ^*. The potential for the D/A pair is

$$2V_{AD} = 3f_A(\Delta r_A)^2 + 3h_A(\Delta\theta_A)^2 + 4f_D(\Delta r_D)^2 + 3(1 + g^2/3)h_D(\Delta\theta_D)^2 \quad (19)$$

To obtain the minimum energy configuration which meets this requirement, eq 19 is differentiated with respect to r and θ and yields eq 20. Thus $r^* = 1.417$ Å, $\theta^* = 104.2°$, and $\phi^* = 114.8°$

$$r^* = (3f_A r^\circ_A + 4f_D r^\circ_D)/(3f_A + 4f_D)$$
$$\theta^* = (h_A\theta^\circ_A + (1 + g^2/3)h_D\theta^\circ_D)/(h_A + (1 + g^2/3)h_D) \quad (20)$$

are obtained. (Interestingly, the ab initio optimum geometry obtained for this system gives $\theta^* = 103.2°$.[3b,30]) The geometric contribution to the classical activation barrier for proton transfer $V^*_{AD} = \Delta H^*_L$. For a self-exchange reaction, $\Delta H^*_L = \Delta G^*_L$ and $\Delta G^*_L \simeq \lambda_L/4$. To evaluate ΔH^*_L, r^* and θ^* are substituted into eq 19, i.e., $\Delta r^*_A = r^\circ_A - r^*_A$, $\Delta\theta^*_A = \theta^\circ_A - \theta^*_A$, etc. Thus $\Delta H^*_L = 6.5$ kcal mol^{-1} is obtained, with only 0.01 kcal mol^{-1} of ΔH^*_L arising from the bond-distance changes. At 298 K, $\kappa_L = \exp(-\Delta H^*_L/RT) \simeq 2 \times 10^{-5}$; the requirement for geometry changes is thus calculated to reduce the exchange rate by a factor of $\sim 10^5$ in this system in a weak-interaction model.[31] Analogous treatments of other geometries are given in the Appendix.

The geometry changes occurring in the organometallic systems in Table I are more complicated than those in the PH_4^+/PH_3 exchange and in the idealized ML_nH/ML_n^- exchanges (Appendix). For the $M(cp)(CO)_3$ series there are changes in both OC–M–CO angles (typically 86° in the anion and 78° in the hydride) and cp–M–CO angles (128° in the anion, 110–125° in the hydride defined with respect to the centroid of the cyclopentadienide ligand).[32,33]

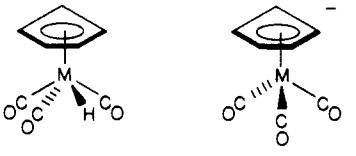

As noted earlier $H_2M(CO)_4$ is pseudooctahedral (nominally 90° L–M–L bond angles, but for M = Fe distinctly distorted toward a tetrahedral $Fe(CO))_4$ unit[16c]) while $HM(CO)_4^-$ is approximately trigonal bipyramidal[16b] (C–M–C equatorial ~117°, C–M–C axial–equatorial ~99°, C–M–C equatorial–axial ~81°, axial–axial 175°). In addition, the spectator ligands are not monatomic and the force constant data needed in evaluating ΔH^*_L are incomplete—the most complicated carbonyl complex to be subjected to detailed analysis being $M(CO)_6$ (Cr, Mo, W).[34] With these complications in mind "geometric barriers" for these systems will be evaluated: When changes in the cp–M–CO angle are neglected, eq A1–A2 may be directly applied to the $M(cp)(CO)_3H/M(cp)(CO)_3^-$ systems and $\Delta H^*_L = 2.0$ kcal mol^{-1}, $\kappa_L = 3 \times 10^{-2}$, and $\theta^* = 82.8°$ are obtained for $h_A = h_D = 0.6$ mdyn Å rad^{-2}. For typical ML_5H/ML_5^- systems with ideal octahedral/trigonal-bipyramidal geometries, $\Delta H^*_L = 26.3$ kcal mol^{-1}, $\kappa_L = 6.5 \times 10^{-20}$, and $\theta^* = 106.7°$ are obtained from eq A1–A2 when h_D and h_A are taken[34] as 0.5 and 0.6 mdyn Å rad^{-2}, respectively. These results are qualitatively in accord with intuition: the ML_5H/ML_5^- systems which require large geometric changes upon proton transfer are calculated to have large ΔH^*_L values and the $M(cp)(CO)_3H/M(cp)(CO)_3^-$ self-exchanges, which require little geometric change upon proton transfer, are calculated to have small ΔH^*_L values. The "geometric barriers" obtained for the ML_5H/ML_5^- (or ML_4H_2/ML_4H^-) systems are, however, much too great to be consistent with the experimentally determined barriers.

The Fluxional Partner. There is ample reason (apart from the large magnitude of the barrier inferred) to distrust the above result for ML_5H/ML_5^- systems. Five-coordinate d^8 systems are fluxional, with equatorial and axial ligands readily interconverting probably via a square-pyramidal geometry in a "Berry twist" mechanism.[35]

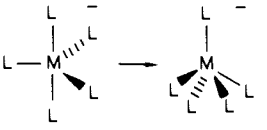

A harmonic treatment of the Berry twist for an $M(CO)_5$ species (via a *flat* square pyramid $\theta = \phi = 90°$) yields a barrier of 60 kcal mol^{-1} ($k_{298} \sim 10^{-31}$ s^{-1}). Yet both $Os(CO)_5$[35] and $Fe(CO)_5$ are known to be fluxional down to very low temperatures ($\Delta G^* \leq 8$ and ~1 kcal mol^{-1}, respectively). For $Fe(CO)_5$ the square-pyramidal form (probable trans C–Fe–C basal angle 164°; $\phi^\circ_A = 98°$[36]) is ≤2 kcal mol^{-1}[37] higher in energy than the equilibrium trigonal-bipyramidal species, consistent with the observed ~1 kcal mol^{-1} barrier to axial–equatorial interconversion.[38] Thus, as has been found for d^0 PF_5,[39] attempts to treat the inversion process with a harmonic model yield barriers a factor of 10 or more greater than is consistent with experiment.[39] Evidently the motion interconverting D_{3h} and C_{4v} geometries is very facile[40] (see Figure 5 in ref 40) for both d^8 and d^0 five-coordinate species.

The facile accessibility of square-pyramidal geometry to d^8 five-coordinate species suggests a reasonable alternative to Scheme II as a reaction pathway for proton self-exchange in these systems.[41] To the extent that the pseudorotation motion in ML_5^- yields a species more closely resembling the hydride in geometry than the trigonal-bipyramidal configuration this process may

(30) del Bene, J., personal communication.
(31) (a) When the quantities in eq 16 are expressed in mdyn Å^{-1}, Å, mdyn rad^{-2}, radians (1 radian = 57.295°), the conversion factor 144 (kcal·mol^{-1})/(mdyn·Å) is useful. (b) In the PH_3/PH_4^+ system the bending frequencies are so high (~1000 cm^{-1}) that substantial tunneling corrections should be applied. Thus this is a poor model for a transition-metal system in which these bending modes are of much lower frequency. It does however offer conceptual simplicity lacking in the lower symmetry multiatomic systems in Table I.
(32) Structures for the $M(cp)(CO)_3^-$ three-legged piano stool have been reported: (a) Feld, R.; Hellner, E.; Klopsch, A.; Dehnicke, K. *Z. Anorg. Allg. Chem.* **1978**, *442*, 172 (M = Cr). (b) Crotty, D. E.; Corey, E. R.; Anderson, T. J.; Glick, M. D.; Oliver, J. P. *Inorg. Chem.* **1977**, *16*, 920 (M = Mo). (c) Adams, M. A.; Folting, K.; Huffman, J. C.; Caulton, K. G. *Inorg. Chem.* **1979**, *18*, 3020 (M = Mo).
(33) Structures of $M(cp)(CO)_3X$ have been described: (a) Bueno, C.; Churchill, M. R. *Inorg. Chem.* **1981**, *20*, 2197 (X = Cl; M = Mo, W). (b) Chaiwasic, S.; Fenn, R. H. *Acta Crystallogr.* **1968**, *B24*, 525 (X = Cl, M = Mo).
(34) (a) $h_D = 0.6$ mdyn Å rad^{-2} is taken from: Jones, L. H.; McDowell, R. S.; Goldblatt, M. *Inorg. Chem.* **1969**, *11*, 2349; Jones, L. H. *Inorganic Vibrational Spectroscopy*; Marcel Dekker: New York, 1971. (b) The value h_A is taken from the equatorial value for $Fe(CO)_5$ given by: Jones, L. H.; McDowell, R. S.; Goldblatt, M.; Swanson, B. I. *J. Chem. Phys.* **1972**, *57*, 2050.
(35) (a) Mann, B. E. *Compr. Organomet. Chem.* **1982**, *3*, 89. (b) In contrast to $H_2Fe(CO)_4$ six-coordinate, carbonyl hydrides are generally stereochemically rigid. Vancea, L.; Graham, W. A. *J. Organomet. Chem.* **1977**, *134*, 219. Yarrow, P.; Ford, P. C. *J. Organomet. Chem.* **1981**, *214*, 115.
(36) Rossi, A. R.; Hoffmann, R. *Inorg. Chem.* **1975**, *14*, 365.
(37) Blyholder, G.; Springs, J. *Inorg. Chem.* **1985**, *24*, 224.
(38) Sheline, R. K.; Mahnke, H. *Angew. Chem., Int. Ed. Engl.* **1975**, *14*, 314.
(39) Holmes, R. R. *Acc. Chem. Res.* **1972**, *5*, 296.
(40) Hoffmann, R.; Howell, J. M.; Muetterties, E. L. *J. Am. Chem. Soc.* **1972**, *94*, 3047.
(41) The pathway discussed here is appropriate when the d^6 acid is stereochemically rigid and thus is applicable to $H_2Ru(CO)_4$, $H_2Os(CO)_4$, $HMn(CO)_4$, etc. but not for $H_2Fe(CO)_4$.

reduce the geometric barrier for proton self-exchange. For example, the proton self-exchange might proceed via a pre-equilibrium formation of the trigonal-bipyramidal isomer as illustrated in Scheme III. As given in detail in the Appendix, incorporation

Scheme III

$$\underset{\text{sq pyr}}{ML_5^-} \rightleftharpoons \underset{\text{trig bipyr}}{(ML_5^-)'}$$

$$(ML_5^-)' + HML_5 \rightleftharpoons [(ML_5^-)'HML_5]$$

$$[(ML_5^-)'HML_5] \overset{k_p'}{\rightleftharpoons} [ML_5H(ML_5^-)']$$

proton transfer

$$[ML_5H(ML_5^-)'] \rightleftharpoons ML_5H + (ML_5^-)'$$

$$(ML_5^-)' \rightleftharpoons ML_5^-$$

of the fluxionality of the d^8 base ($HM(CO)_4^-$) suggests a geometric barrier $\Delta H^*_L \simeq 5$ kcal mol^{-1} for HML_5/ML_5^- proton self-exchange. This is greater than that estimated (2 kcal mol^{-1}) for the $M(cp)(CO)_3H/M(cp)(CO)_3^-$ systems, but not as great as is predicted from a harmonic-oscillator treatment of the equilibrium bond-angle difference between ML_5H and ML_5^-. Thus these considerations suggest a $\sim$3 kcal mol^{-1} greater barrier (factor of $\sim 10^2$ in rate) for ML_5H/ML_5^- self-exchanges than for $M(cp)(CO)_3H/M(cp)(CO)_3^{5-}$ self-exchanges, if all other factors are the same. The measured rate constants for $W(cp)(CO)_3^-$ and $HOs(CO)_4^-$ exchanges (Table I) exhibit this trend.[42]

The above treatment, which involved a pre-equilibrium "isomerization" of ML_5^- followed by harmonic distortion of the square-pyramidal $ML_5^-|HML_5$ pair (Scheme III), or a related approach is likely to be appropriate in a number of organometallic systems. Simple proton self-exchanges necessarily involve a coordination number change of 1 at the metal. Since coordination numbers 5, 7, 8, and 9 are generally fluxional to a degree, there are a very large number of systems in which the fluxionality of either the metal base or metal hydride may offer a kinetically significant pathway to the proton self-exchange (or net) reaction. It seems possible that, at minimum, empirical rules based on the fluxional barrier manifested by the fluxional partner might be used to rationalize (and predict) relative self-exchange barriers in appropriately selected systems.[43] More ambitious is the quantitative treatment of fluxionality in these systems—a subject that has been addressed in a limited way in both molecular orbital and (most recently) molecular mechanics frameworks. Indeed the recent work of Lauher[44] appears especially promising in this regard.

Finally, it is worth noting that, while the quantitative treatment of geometric changes is expected to be extremely challenging in most systems, the use of the weak-interaction model makes it possible to focus (albeit perhaps artificially) on the geometric changes attending proton transfer as a separate issue. For nonfluxional systems (both partners rigid) the geometric barriers are predicted to increase with the magnitude of the angular changes and with the bending force constants. For fluxional systems, the geometric barrier may correlate with the polytopal barrier of the fluxional partner. These predictions need to be tested. Systems in which there is no geometry change on H^+ transfer should be examined to see if the intrinsic self-exchange barriers are reduced compared to the fastest systems reported to date. Fluxional barriers for, e.g., d^8 ML_5^- "bases" need to be evaluated and compared with proton self-exchange barriers in the ML_5H/ML_5^- systems.

Table IV. Comparison of Calculated and Experimental Rate Parameters for the $Mo(cp)(CO)_3H/D + Mo(cp)(CO)_3^-$ Self-Exchange at 298 K[a] (see also Table III)

	H		D	
	calcd	obsd	calcd	obsd
H_{AB} (kcal mol^{-1})	(2.0)[b]		(2.0)[b]	
U (kcal mol^{-1})	4.80		5.83	
ΔH^*_L (kcal mol^{-1})	2.0		2.0	
λ_{out} (kcal mol^{-1})	4.69		4.61	
k (M^{-1} s^{-1})	3×10^3	2.5×10^3	2×10^2	6.7×10^2
ΔH^* (kcal mol^{-1})	6.0	5.3 (3)[c]	7.0	6.3 (5)[c]
ΔS^* (cal mol^{-1} K^{-1})	−23	−25.3 (12)[c]	−25	−24.0 (8)[c]

[a] Calculated parameters refer to the maxima in Figure 4. The observed values are taken from ref 13; numbers in parentheses are estimated standard deviations given in ref 13. [b] Not calculated. [c] Actually $\Delta H^\ddagger$ and $\Delta S^\ddagger$. Since ν_{el} is taken as 10^{13} s^{-1}, the difference between $\Delta H^\ddagger$ and ΔH^* or $\Delta S^\ddagger$ and ΔS^* is negligible.

Comparisons with Experimental Results

As is summarized in Table III a weak-interaction exchange rate constant of 8.5×10^4 M^{-1} s^{-1} (with $H_{AB} \sim 2$ kcal mol^{-1}) is calculated for a second transition series hydrido complex in the absence of geometry changes. Incorporation of geometry changes may further reduce the rate by a factor of 3×10^2 and increase ΔH^* by 2.0 kcal mol^{-1} in the $M(cp)(CO)_3H$ series. Thus for $Mo(cp)(CO)_3H$ assuming $H_{AB} = 2$ kcal mol^{-1}, the values $k_H = 3 \times 10^3$ M^{-1} s^{-1} at 298 K, $\Delta H^* = 6.0$ kcal mol^{-1}, and $\Delta S^* = -23$ cal deg^{-1} mol^{-1} are obtained. In Table IV these are compared with the data of Edidin et al.:[13] $k_H = 2.5 \times 10^3$ M^{-1} s^{-1}, $\Delta H^\ddagger = 5.3$ kcal mol^{-1}, and $\Delta S^\ddagger = -25.3$ cal deg^{-1} mol^{-1}. The reported kinetic isotope effect is $k_H/k_D = 3.7$ and the calculated value is $\sim$15. For the $H_2M(CO)_4$ exchanges, geometry changes might reduce the rate by 5×10^3 at 298 K and increase ΔH^* by 5 kcal mol^{-1}. Thus with the second transition series model (Figures 3 and 4), the $H_2Ru(CO)_4$ or $HTc(CO)_5$ exchange is predicted to have $k_H \sim 20$ M^{-1} s^{-1}, $\Delta H^* \sim 9$ kcal mol^{-1}, and $\Delta S^* = -23$ cal deg^{-1} mol^{-1} (if $H_{AB} = 2$ kcal mol^{-1}). Unfortunately self-exchange data for only $H_2Fe(CO)_4$, $k_H \sim 1.3 \times 10^3$ M^{-1} s^{-1}, and $H_2Os(CO)_4$, $k_H = 0.07$ M^{-1} s^{-1}, at 298 K are available.[13,10] From the comparisons in Table IV we conclude that the weak-interaction model in the partially adiabatic limit can yield rates and activation parameters close enough to the observed values that the model—and proton-transfer mechanism—merit serious consideration for the metal hydride systems.

The calculated ($k_H/k_D \sim 15$ at 298 K) and observed[13] ($k_H/k_D = 3.7$ at 298 K) kinetic isotope effects in Table IV also merit comment. Within the weak-interaction model the kinetic isotope effect for the self-exchange reaction is largely determined by the factor $\kappa_u(FC)_{0,0}^r$ (see Figure 4) and so is extremely sensitive to the form of the repulsive factor used. In view of the uncertainties in the repulsive parameters (and in the form of the prefactor for a partially adiabatic reaction[21c]) the rate-ratio discrepancy is not a serious one: a smaller isotope effect would be calculated if κ_u^r were increased ("softer" repulsive potential). However, the pattern expected for the activation parameters for the isotope effect has more significance than the rate ratio: As noted earlier, within the weak-interaction model, ΔH^* is predicted to be more positive, and ΔS^*, more negative, for the deuterio self-exchange than for the protio self-exchange. The expected pattern is found for ΔH^*. However, the observed $\Delta S^\ddagger$ is somewhat more negative for the protio self-exchange, $\Delta S^*_H(obsd) < \Delta S^*_D(obsd)$, while $\Delta S^*_D(calcd) < \Delta S^*_H(calcd)$. On the basis of this criterion, the $M(cp)(CO)_3$ proton self-exchanges do not appear to be in accord with the weak-interaction treatment. However, the trends in the $\Delta S^\ddagger$ values are within the experimental error in the measurements. It remains to be seen whether or not this isotope effect pattern is a general feature of transition-metal-based proton self-exchanges.

(42) (a) It is also worth mentioning the $Mn(CO)_5H/Mn(CO)_5^-$ self-exchange, in which the idealized geometric changes assumed above are observed.[24c,42b] While the self-exchange has not been studied, the studies of Edidin et al. suggest very similar barriers for proton transfer from $H_2Fe(CO)_4$ and $HMn(CO)_5$ to substituted anilines at zero driving force.[13] Both barriers are considerably greater than that for $W(cp)(CO)_3H$. (b) Frenz, B. A.; Ibers, J. A. *Inorg. Chem.* **1972**, *11*, 1109.

(43) (a) For example, in the d^8 ML_5 series (L = $P(OCH_3)_3$) the pseudorotational barrier (7–10 kcal mol^{-1}) has been found to follow the order Fe > Os > Ru, Co > Fe > Ni, etc.[43b,c] (b) Jesson, J. P.; Muetterties, E. L. In *Dynamic Nuclear Magnetic Resonance Spectroscopy*; Jackman, L. M., Cotton, F. A., Eds.; Academic: New York, 1975; p 253. (c) English, A. D.; Ittel, S. D.; Tolman, C. A.; Meakin, P.; Jesson, J. P. *J. Am. Chem. Soc.* **1977**, *99*, 117.

(44) Lauher, J. *J. Am. Chem. Soc.* **1986**, *108*, 1521.

Within the weak-interaction model the proton-transfer rate falls off extremely rapidly with reactant separation (see Figures 2–4). The rates are thus expected to be extremely sensitive to factors which prevent close M–H/M⁻ contacts. Thus it is worth noting that extraordinary rate sensitivity to the steric bulk of the hydride complex and the base has been experimentally observed for two hydrido systems in which extremely bulky phosphine ligands are incorporated.[45] Such sensitivity to steric effects does not, of course, require a weak-interaction model but is consistent with any model requiring fairly close M–H/M⁻ contacts.

Concluding Remarks

The relatively large intrinsic barriers to proton transfer between transition-metal centers have been attributed previously[10,15] to the large nuclear and electronic configuration changes attending proton transfer. Here we have applied a weak-interaction, golden-rule model to proton self-exchange reactions of metal hydride complexes. Within this model the rate constant is a product of terms for assembling hydride and conjugate base at the correct orientation and distance, a classical reaction frequency, an electron–proton reaction probability, and classical nuclear factors deriving from the requirement for reorganization of ancillary ligand and solvent modes prior to proton transfer (assumed to be fast). Thus the nuclear configuration changes (largely angular in nature) contribute a classical activation barrier, which may be evaluated, in principle, from a knowledge of hydride and conjugate base structures, vibrational spectra, and fluxional properties. Within this model no activation barrier arises from the electronic configuration changes for the systems considered; the reactions are electronically adiabatic with electronic reorganization following nuclear reorganization smoothly (but this is not necessarily always the case[46]). Although many approximations were made in order to evaluate the various rate-attenuating factors, the results obtained are sufficiently close to experimentally determined parameters that this weak-interaction model merits serious consideration for reactions of this class. General application of the model to transition-metal centers will, however, require a better understanding of the fluxional behavior of these complexes; it is hoped that such an understanding may emerge from molecular mechanics calculations. In addition, expressions accurately describing the distance dependence of both the electron–electron repulsion and the reactant–product electronic coupling are required if reliable rate calculations are to be made.

Acknowledgment. Helpful discussions with Drs. M. A. Andrews, B. Brunschwig, R. M. Bullock, J. R. Norton, R. A. Marcus, and J. Ulstrup are gratefully acknowledged and we thank J. R. Norton for providing us with ref 13 prior to publication. This research was carried out at Brookhaven National Laboratory under contract DE-AC02-76CH00016 with the U.S. Department of Energy and supported by its Division of Chemical Sciences, Office of Basic Energy Sciences.

Appendix

(1) Franck–Condon Treatments of the Geometry Changes. (a) Octahedral Hydride/Trigonal-Bipyramidal Base. The structural differences between D and D′ and A and A′ (see Scheme II) define the angular deformations required prior to the proton transfer between D* and A* in the self-exchange reaction. For proton transfer between an octahedral hydride and a trigonal-bipyramidal base, the (essentially normal mode) motion required in D is a simultaneous compression of L–M–H angles and opening of L–M–L in-plane angles. Thus as L_1–M–H and L_2–M–H angles

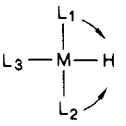

decrease by $\Delta\theta_D$, the L_1–M–L_3 and L_3–M–L_2 angles increase by $\Delta\theta_D$ and

$$2V_D = 4h_D(\Delta\theta_D)^2$$

where the bending force constant has been assumed to be the same for the L–M–L and L–M–H angles. The (essentially normal mode) motion required in the proton acceptor involves compression of two angles. As angles L_1–M–L_3 and L_2–M–L_3 decrease

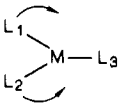

by $\Delta\theta_A$, the angle L_1–M–L_2 increases by $2\Delta\theta_A$ and

$$2V_A = 6h_A(\Delta\theta_A)^2$$

As discussed for the PH_4^+/PH_3 exchange, minimization of the energy $V_{AD} = V_A + V_D$ gives θ^*, defined here as the L_1–M–L_3 angle. From θ^* and the definition of V^*_{AD}, expressions for ΔH^*_L and λ_L are obtained with $\bar{h}$, the effective bending force constant defined as shown.

$$\theta^* = (3h_A\theta^\circ_A + 2h_D\theta^\circ_D)/(3h_A + 2h_D) \qquad \text{(A1)}$$

$$\Delta H^*_L = (\bar{h}/2)(\theta^\circ_A - \theta^\circ_D)^2$$

where

$$\bar{h} = 2(3h_A)(2h_D)/(3h_A + 2h_D) \qquad \text{(A2)}$$

and

$$\lambda_L = 3h_A(\theta^\circ_A - \theta^\circ_D)^2 + 2h_D(\theta^\circ_A - \theta^\circ_D)^2 = \Delta H^*_L\left(4 + \frac{(3h_A - 2h_D)^2}{h_D h_A}\right)$$

(b) Octahedral Hydride/Square-Pyramidal Base. In the base

octahedral square-pyramidal

there is one axial site and there are four basal sites. The proton is transferred to the vacant axial site on ML_5^-.

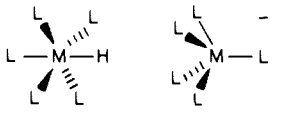

The ML_5^- basal L–M–basal L angle is denoted θ_A and the axial L–M–basal L angle is denoted ϕ_A. The corresponding angles in ML_5H are denoted θ_D and ϕ_D, respectively. When fourfold symmetry is conserved, the angles ϕ and θ are related through

$$\sin(\phi) = \sqrt{2}\sin(\theta/2)$$

$$\text{and } \Delta\phi \simeq \frac{\sqrt{2}}{2}\left(\frac{\cos(\theta/2)}{\cos(\phi)}\right)\Delta\theta \simeq g\Delta\theta$$

$$\text{with } g = \frac{\sqrt{2}}{2}\left(\frac{\cos(\theta/2)}{\cos(\phi)}\right) \qquad \text{(A3)}$$

As found earlier for PH_4^+/PH_3 a simple bending motion is required at each center to attain θ^* and ϕ^*: For ML_5H/ML_5^-, because $\phi_D = 90°$ (octahedral) and $\phi^\circ_A > 90°$ (square pyramidal), four ϕ_D angles increase by $\Delta\phi_D$, four ϕ_D angles decrease by $\Delta\phi_D$,

(45) (a) Thaler, E.; Folting, K.; Huffmann, J. C.; Caulton, K. G. *Inorg. Chem.* **1987**, *26*, 374. (b) Hanckel, J. M.; Darensbourg, M. Y. *J. Am. Chem. Soc.* **1983**, *105*, 6979.

(46) It can be shown that for ML_nH/ML_n^- pairs which are 18-electron species there should be good electronic correlation between acid and base, that is proton transfer is orbital-symmetry-allowed in a Woodward–Hoffmann sense. For example, the d_{z^2} orbital in a d^8 square-pyramidal ML_5^- base provides the electron pair to which H^+ is transferred; in ML_5H the combination of metal d_{z^2} with the hydrogen 1s orbital gives a filled bonding σ orbital and an empty σ^* orbital, d_{z^2}. Thus, proton transfer occurs on a single electronic surface for 18-electron reactants.

and four θ_D angles decrease by $\Delta\theta_D$. In addition four ϕ_A angles decrease by $\Delta\phi_A$ and four θ_A angles increase by $\Delta\theta_A$ to θ^*. From these considerations eq A4 and A5 are obtained with, as above, a single bending force constant assumed for both L–M–L and H–M–L bending:

$$2V_{AD} = 4h_A(1 + g_A^2)\Delta\theta_A^2 + 4h_D(1 + 2g_D^2)\Delta\theta_D^2 \quad (A4)$$

$$\theta^* = \frac{4h_A(1 + g_A^2)\theta^\circ_A + 4h_D(1 + 2g_D^2)\theta^\circ_D}{4h_A(1 + g_A^2) + 4h_D(1 + 2g_D^2)} \quad (A5)$$

(2) Pathways Involving Fluxional Species. Rather detailed knowledge of the potential-energy surface for pseudorotation is required if this fluxional feature is to be incorporated into the model correctly. The following questions arise: (1) Is the square-pyramidal ML_5^- form (in which the axial/equatorial identity is lost) an intermediate or a transition state? If the square-pyramidal species is an intermediate, a pre-equilibrium step (K_{spy}; ΔH°_{spy}) to give this species can be incorporated in the mechanistic scheme. (2) What are the angles in the square-pyramidal form? If the trans L–M–L basal angle is 180° the square-pyramidal form is perfectly matched to an octahedral hydride and no further deformation is required. However, the trans basal angle is generally <180° in d^8 structures which have been characterized. (3) Provided that the trans basal angle of the square-pyramidal ML_5^- species is known, how is the geometry difference between this form (spy-ML_5^-) and the octahedral HML_5 to be taken into account? Flattening of the square pyramid to a basal angle of 180° could be as facile as the Berry motion; that is, the effective bending force constant could be quite small, perhaps 0.01 mdyn Å rad^{-2}. In such a situation the proton exchange would occur through transfer from the hydride in its equilibrium geometry to a base having the hydride's spectator ligand geometry, with ΔH^*_L reflecting only the cost of geometric rearrangement on the base ML_5^-. On the other hand, the force constant for flattening of the square pyramid which effects the pseudorotation need not be as small as for the Berry motion: Hoffman's surface for PH_5[40] indicates that such a motion is harmonic and energetic, with the bending force constant perpendicular to the pseudorotation deformation being ~30 times greater than along the pseudorotation deformation. In such a case, knowledge of the geometry of spy-ML_5^- is critical.

For the sake of discussion, one specific set of constraints is considered. These are illustrated in Scheme IV. The rearrangement of the base ML_5^- is treated as a rapid pre-equilibrium (K_{spy}) and proton exchange is taken to occur between the open apical site on square-pyramidal ML_5^-, spy-ML_5^-, and rigid octahedral ML_5H with ΔH^*_L determined by ΔH°_{spy} and $(\Delta H^*_L)'$ arising from the ca. 8° out-of-plane bend required for spy-ML_5^- and HML_5 angles. From the bending force constant estimate[34] 0.6 mdyn Å rad^{-2} and eq A4 and A5 $(\Delta H^*_L)'$ contributes ~4 kcal mol^{-1} to ΔH^*. With $K_{spy} \simeq 0.2$, requirements for angular reorganization reduce the ML_5H/ML_5^- exchange rate by a factor of 5×10^3 at 298 K, with a total contribution of ~5 kcal mol^{-1} to ΔH^*.

Scheme IV

$$\underset{\text{oct}}{ML_5H}|\underset{\text{tb}}{ML_5^-} \overset{K_{spy}}{\rightleftharpoons} \underset{\text{oct}}{ML_5H}|\underset{\text{spy}}{ML_5^-}$$

$$\underset{\text{oct}}{ML_5H}|\underset{\text{spy}}{ML_5^-} \overset{(\Delta H^*_L)'}{\rightleftharpoons} (ML_5H|ML_5^-)^*$$

$$(ML_5H|ML_5^-)^* \rightleftharpoons (ML_5^-|HML_5)^*$$

$$(ML_5^-|HML_5)^* \rightarrow \rightarrow \underset{\text{tb}}{ML_5^-}|\underset{\text{oct}}{ML_5H}$$

Synthesis, Structure, Dynamic Behavior, and Reactivity of Rhenium Phosphido Complexes $(\eta^5\text{-}C_5H_5)Re(NO)(PPh_3)(\dot{P}R_2)$: The "Gauche Effect" in Transition-Metal Chemistry

William E. Buhro, Bill D. Zwick, Savas Georgiou, John P. Hutchinson, and J. A. Gladysz*

Contribution from the Department of Chemistry, University of Utah, Salt Lake City, Utah 84112. *Received August 31, 1987*

Abstract: Reactions of $(\eta^5\text{-}C_5H_5)Re(NO)(PPh_3)(X)$ (X = OTs (OSO_2-*p*-Tol), OTf (OSO_2CF_3)) with PR_2H (R = Ph (**a**), *p*-Tol (**b**), Et (**c**), *t*-Bu (**d**)) give secondary phosphine complexes $[(\eta^5\text{-}C_5H_5)Re(NO)(PPh_3)(PR_2H)]^+X^-$ (**2a**-TsO$^-$, **2b**-TsO$^-$, **2c**-TfO$^-$, **2d**-TfO$^-$; 87–96%). Reactions of **2a–d**-X$^-$ with *t*-BuO$^-$K$^+$ give phosphido complexes $(\eta^5\text{-}C_5H_5)Re(NO)(PPh_3)(PR_2)$ (**4a–d**; 79–99%). Optically active, configurationally stable (+)-(*S*)-**4b** is analogously prepared. NMR experiments show **4a–d** to have very low PR_2 phosphorus inversion barriers (12.6–14.9 kcal/mol). The rapid alkylation of **4a** by CH_2Cl_2 to give $[(\eta^5\text{-}C_5H_5)Re(NO)(PPh_3)(PPh_2CH_2Cl)]^+Cl^-$ (79%) shows the PR_2 phosphorus to be highly nucleophilic, and **4a** and **4d** are easily oxidized (O_2, PhIO) to phosphine oxides $(\eta^5\text{-}C_5H_5)Re(NO)(PPh_3)(P(=O)R_2)$ (34–60%). The X-ray crystal structures of **4a** and **4d** show that the PR_2 phosphorus lone pairs make 59–60° torsion angles with the rhenium d orbital HOMO. It is proposed that avoided overlap between these orbitals ("gauche effect") is an important Re–PR_2 conformation-determining factor. This proposal is supported by extended-Hückel MO calculations on the model compound $(\eta^5\text{-}C_5H_5)Re(NO)(PH_3)(PH_2)$.

As exemplified by the classic Dewar–Chatt–Duncanson model for transition metal–olefin complexes,[1] bonds between transition metals and unsaturated ligands commonly consist of two components: (1) donation of ligand electrons to metal σ-acceptor orbitals, and (2) donation of metal d electrons to ligand π-acceptor orbitals. These interactions are shown schematically in Figure 1. The latter, generally termed back-bonding,[2,3] has important

(1) (a) Dewar, M. J. S. *Bull. Soc. Chim. Fr.* **1951**, *18*, C71. (b) Chatt, J.; Duncanson, L. A. *J. Chem. Soc.* **1953**, 2939.

(2) Collman, J. P.; Hegedus, L. S.; Norton, J. R.; Finke, R. G. *Principles and Applications of Organotransition Metal Chemistry*; University Science Books: Mill Valley, CA, 1987; pp 37–54.

0002-7863/88/1510-2427$01.50/0 © 1988 American Chemical Society